

## Nonlinear rheology of linear polymer melts: Modeling chain stretch by interchain tube pressure and Rouse time

Manfred H. Wagner\* and Víctor H. Rolón-Garrido

Chair of Polymer Engineering and Physics, Berlin Institute of Technology (TU Berlin),  
Fasanenstrasse 90, D-10623 Berlin, Germany

(Received May 13, 2009)

### Abstract

In flows with deformation rates larger than the inverse Rouse time of the polymer chain, chains are stretched and their confining tubes become increasingly anisotropic. The pressures exerted by a polymer chain on the walls of an anisotropic confinement are anisotropic and limit chain stretch. In the Molecular Stress Function (MSF) model, chain stretch is balanced by an interchain pressure term, which is inverse proportional to the 3<sup>rd</sup> power of the tube diameter and is characterized by a tube diameter relaxation time. We show that the tube diameter relaxation time is equal to 3 times the Rouse time in the limit of small chain stretch. At larger deformations, we argue that chain stretch is balanced by two restoring tensions with weights of 1/3 in the longitudinal direction of the tube (due to a linear spring force) and 2/3 in the lateral direction (due to the nonlinear interchain pressure), both of which are characterized by the Rouse time. This approach is shown to be in quantitative agreement with transient and steady-state elongational viscosity data of two monodisperse polystyrene melts without using any nonlinear parameter, *i.e.* solely based on the linear-viscoelastic characterization of the melts. The same approach is extended to model experimental data of four styrene-butadiene random copolymer melts in shear flow. Thus for monodisperse linear polymer melts, for the first time a constitutive equation is presented which allows quantitative modeling of nonlinear extension and shear rheology on the basis of linear-viscoelastic data alone.

**Keywords :** constitutive equation, monodisperse polymer, Doi-Edwards model, MSF model, tube diameter relaxation, Rouse relaxation

### 1. Introduction

In elongational flow, the Doi-Edwards (DE) model with the so-called independent alignment assumption predicts an upper limit of the tensile stress equal to 5 times the plateau modulus,  $G_N$ . This limiting stress results from the assumption of instantaneous chain retraction and therefore the absence of any chain stretching. In the DE model, the macroscopic stress is a consequence of chain orientation only, resulting in a scaling of the steady-state elongational viscosity at strain rates  $\dot{\epsilon}$  larger than the inverse reptation time according to  $\dot{\epsilon}^{-1}$ . Relaxing the assumption of instantaneous chain retraction, various reptation-based models have invoked chain stretch when the deformation rate is larger than the inverse Rouse time  $\tau_R$  of the chain, but quantitative agreement with experimental data was not achieved.

In contrast to the DE scaling, elongational viscosity measurements of Bach *et al.* (2003) on narrow molar mass dis-

tribution polystyrene melts have revealed that the elongational viscosity scales approximately with  $\dot{\epsilon}^{-1/2}$ . Marrucci and Ianniruberto (2004) have introduced an interchain pressure term arising from lateral forces between the chain and the tube wall into the DE model to account for this effect, leading to a specific tube diameter relaxation time, which limits chain stretching. However, their analysis was restricted to scalar arguments and to the steady-state viscosity. A full constitutive equation, which describes time-dependent as well as steady-state rheology of nearly monodisperse polymer melts was presented by Wagner *et al.* (2005), and predictions are in excellent agreement with the elongational viscosity data of Bach *et al.* (2003), Hassager (2004), and Nielsen *et al.* (2006).

The tube diameter relaxation time as introduced by Marrucci and Ianniruberto (2004) has been expected to be proportional to the Rouse relaxation time. However, the exact value of the proportionality constant remained elusive, and so far, the tube diameter relaxation time has been used as a fit parameter. By considering the limit of small chain stretch, we show that in the melt, the tube diameter relaxation time is equal to 3 times the Rouse stretch relaxation

\*Corresponding author: manfred.wagner@tu-berlin.de  
© 2009 by The Korean Society of Rheology

time of the chain, and we propose a combination of Rouse relaxation and tube diameter relaxation in agreement with experimental evidence at larger deformations. We also extend this approach to an analysis of shear viscosity data of four styrene-butadiene random copolymer melts (Boukany *et al.*, 2009).

## 2. Experimental Data

The elongational data discussed are those reported by Bach *et al.* (2003) and Hassager (2004) on nearly monodisperse polystyrene (PS) melts. Polymer characterization and spectra of 2 nearly monodisperse polystyrene melts are summarized in Table 1. The Rouse time  $\tau_R$  and the longest relaxation time  $\tau_w$  (identified with the reptation time here) were calculated according to well-known relations (Osaki *et al.*, 1982; Menezes and Graessley, 1982; Takahashi *et al.*, 1993; Isaki *et al.*, 2003),

$$\tau_R = \frac{12M\eta_0}{\pi^2 \rho RT} \left(\frac{M_c}{M}\right)^{2.4} \quad (1)$$

and

$$\tau_w = J_{e0} \eta_0 \quad (2)$$

$M_c$  of polystyrene was taken as 35,000 g/mol.

The experimental shear data analyzed are those reported by Boukany *et al.* (2009) on four styrene-butadiene random copolymer (SBR) melts, denoted as SBR100K, SBR170K, SBR250K and SBR500K with molar masses from 94.8 kg/mol to 497 kg/mol. The linear-viscoelastic parameters and the molecular characterization of the samples are summarized in Table 2. The Rouse times of the

**Table 1.** Molecular characterization [(Nielsen *et al.* 2006) and discrete relaxation spectra (relaxation moduli  $g_i$  and relaxation times  $\lambda_i$ ) of PS samples at 130°C].  $\tau_a$  is the tube diameter relaxation time as determined by Wagner *et al.* (2005)

PS200K		PS390K	
$M_w = 200,000$ g/mol		$M_w = 390,000$ g/mol	
$M_w/M_n = 1.04$		$M_w/M_n = 1.06$	
$J_e^0 = 1.16 \times 10^{-5}$ [Pa <sup>-1</sup> ]		$J_e^0 = 1.50 \times 10^{-5}$ [Pa <sup>-1</sup> ]	
$\eta_0 = 8.26 \times 10^7$ [Pa.s]		$\eta_0 = 7.57 \times 10^8$ [Pa.s]	
$\tau_R = 91.5$ s		$\tau_R = 329$ s	
$\tau_w = 961$ s		$\tau_w = 11351$ s	
$\tau_a = 384$ s		$\tau_a = 1462$ s	
$g_i$ [Pa]	$\lambda_i$ [s]	$g_i$ [Pa]	$\lambda_i$ [s]
$2.38 \times 10^5$	$4.75 \times 10^{-1}$	$4.63 \times 10^5$	$1.04 \times 10^{-1}$
$3.71 \times 10^4$	$5.29 \times 10^0$	$7.79 \times 10^4$	$1.07 \times 10^0$
$2.71 \times 10^4$	$1.96 \times 10^1$	$3.00 \times 10^4$	$9.70 \times 10^0$
$5.46 \times 10^4$	$9.20 \times 10^1$	$2.55 \times 10^4$	$5.16 \times 10^1$
$4.96 \times 10^4$	$4.43 \times 10^2$	$3.33 \times 10^4$	$2.35 \times 10^2$
$4.33 \times 10^4$	$1.26 \times 10^3$	$4.31 \times 10^4$	$1.14 \times 10^3$
		$5.15 \times 10^4$	$5.97 \times 10^3$
		$2.28 \times 10^4$	$1.71 \times 10^4$

melts are those published by the authors.

## 3. The Doi-Edwards Model

When introducing the tube model, Doi and Edwards

**Table 2.** Molecular characterization (Boukany *et al.* 2009) and relaxation spectra (relaxation moduli  $g_i$  and relaxation times  $\lambda_i$ ) at 23°C of SBR copolymers

SBR(100K)		SBR(170K)		SBR(250K)		SBR(500K)	
$M_w = 94.8$ kg/mol		$M_w = 174$ kg/mol		$M_w = 250$ kg/mol		$M_w = 497$ kg/mol	
$M_w/M_n = 1.05$		$M_w/M_n = 1.07$		$M_w/M_n = 1.04$		$M_w/M_n = 1.19$	
$J_e^0 = 3.782 \times 10^{-6}$ Pa <sup>-1</sup>		$J_e^0 = 4.625 \times 10^{-6}$ Pa <sup>-1</sup>		$J_e^0 = 3.892 \times 10^{-6}$ Pa <sup>-1</sup>		$J_e^0 = 3.387 \times 10^{-6}$ Pa <sup>-1</sup>	
$\eta_0 = 7.778 \times 10^6$ Pa.s		$\eta_0 = 6.05 \times 10^7$ Pa.s		$\eta_0 = 1.252 \times 10^8$ Pa.s		$\eta_0 = 9.036 \times 10^8$ Pa.s	
$\tau_R = 1.1$ s		$\tau_R = 2.3$ s		$\tau_R = 4.1$ s		$\tau_R = 13$ s	
$Z = 24$		$Z = 53$		$Z = 76$		$Z = 160$	
$g_i$ [Pa]	$\lambda_i$ [s]	$g_i$ [Pa]	$\lambda_i$ [s]	$g_i$ [Pa]	$\lambda_i$ [s]	$g_i$ [Pa]	$\lambda_i$ [s]
$2.222 \times 10^5$	$5.767 \times 10^{-3}$	$6.464 \times 10^5$	$1.393 \times 10^{-3}$	$1.008 \times 10^5$	$7.750 \times 10^{-3}$	$3.795 \times 10^4$	$5.680 \times 10^{-2}$
$7.308 \times 10^4$	$6.275 \times 10^{-2}$	$2.959 \times 10^4$	$6.216 \times 10^2$	$5.244 \times 10^4$	$8.242 \times 10^{-2}$	$1.014 \times 10^5$	$6.258 \times 10^{-3}$
$9.648 \times 10^4$	$3.980 \times 10^{-1}$	$6.577 \times 10^4$	$3.834 \times 10^{-2}$	$7.108 \times 10^4$	$5.584 \times 10^{-1}$	$4.810 \times 10^4$	$3.194 \times 10^{-1}$
$1.276 \times 10^5$	$2.369 \times 10^0$	$6.850 \times 10^4$	$2.395 \times 10^{-1}$	$1.012 \times 10^5$	$3.595 \times 10^0$	$6.305 \times 10^4$	$1.728 \times 10^0$
$1.681 \times 10^5$	$1.497 \times 10^1$	$8.955 \times 10^4$	$1.297 \times 10^0$	$1.476 \times 10^5$	$2.413 \times 10^1$	$7.846 \times 10^4$	$8.209 \times 10^0$
$1.269 \times 10^5$	$3.873 \times 10^1$	$1.138 \times 10^5$	$6.454 \times 10^0$	$2.475 \times 10^5$	$2.133 \times 10^2$	$1.019 \times 10^5$	$3.766 \times 10^1$
		$1.504 \times 10^5$	$3.295 \times 10^1$	$9.435 \times 10^4$	$7.258 \times 10^2$	$1.444 \times 10^5$	$1.881 \times 10^2$
		$2.469 \times 10^5$	$1.470 \times 10^2$			$2.031 \times 10^5$	$1.051 \times 10^3$
						$1.709 \times 10^5$	$3.852 \times 10^3$

assumed that the diameter  $a_0$  of the tube is not changed even by large non-linear deformations, or equivalently that the tension in the deformed macromolecular chain remains constant and equal to its equilibrium value (Doi and Edwards, 1986). The extra stress tensor  $\boldsymbol{\sigma}(t)$  is then a consequence of the orientation of tube segments due to the flow. The resulting constitutive equation is of the single integral form,

$$\boldsymbol{\sigma}(t) = \int_{-\infty}^t m(t-t') \mathbf{S}_{\text{DE}}^{\text{IA}}(t, t') dt' \quad (3)$$

if the tube segments are assumed to align independently of each other in the flow field (the ‘‘Independent Alignment (IA)’’ approximation).  $m(t-t')$  is the memory function with  $m(t-t') = \sum (g_i/\lambda_i) e^{-(t-t')/\lambda_i}$ , and the relative strain measure  $\mathbf{S}_{\text{DE}}^{\text{IA}}$  is given by

$$\mathbf{S}_{\text{DE}}^{\text{IA}}(t, t') \equiv 5 \left\langle \frac{\mathbf{u}' \mathbf{u}'^T}{u'^2} \right\rangle_o = 5 \mathbf{S}(t, t') \quad (4)$$

$\mathbf{S}$  is the relative second order orientation tensor. The bracket denotes an average over an isotropic distribution of unit vectors  $\mathbf{u}(t')$  at time  $t'$ , and can be expressed as a surface integral over the unit sphere,

$$\langle \dots \rangle_o \equiv \frac{1}{4\pi} \int \int \int [\dots] \sin \theta_o d\theta_o d\phi_o \quad (5)$$

At the observation time  $t$ , the unit vectors are deformed to vectors  $\mathbf{u}'$ , which are calculated from the affine deformation hypothesis (with  $\mathbf{F}^{-1}(t, t')$  as the relative deformation gradient tensor) as

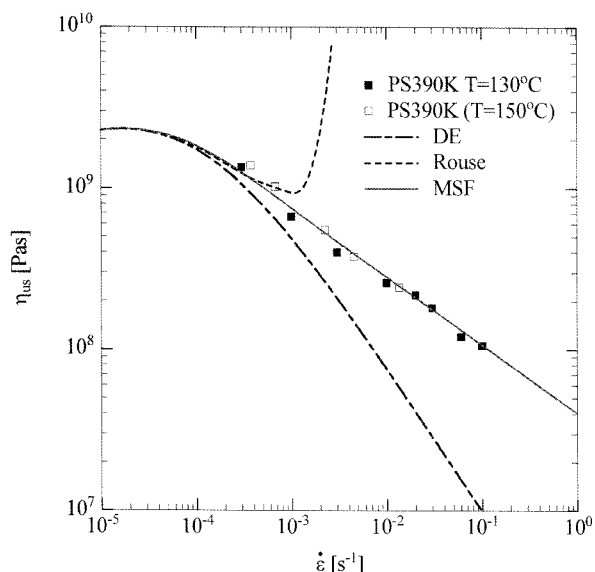


**Fig. 1.** Comparison of steady-state elongational viscosity data of PS390K measured at 130°C (full symbols), and at 150°C (shifted to 130°C, open symbols), to predictions by DE theory (dash-dotted line), Eq. (3), Rouse stretch (dotted line), Eq. (10), and MSF model (full line) according to evolution equation (17).

$$\mathbf{u}(t, t') = \mathbf{F}^{-1}(t, t') \cdot \mathbf{u}(t') \quad (6)$$

$u'$  indicates the length of the vector  $\mathbf{u}'$ .

As the stress is assumed to be due to orientation of tube segments only, the DE model does not account for any strain hardening. This is demonstrated in Fig. 1, where predictions of the DE model are compared to the steady-state elongational data of PS390K. As expected, prediction and data deviate increasingly with increasing strain rate, as the DE prediction scales with  $\dot{\epsilon}^{-1}$ , while the data scale approximately with  $\dot{\epsilon}^{-1/2}$ .

#### 4. Modeling Chain Stretch

Doi and Edwards (Doi and Edwards, 1986) added a stretch process with a stretch  $\lambda$  of the tube segments to their model in order to explain the discrepancies of the DE theory at start-up of shear and extensional flows. Pre-averaging the stretch, *i.e.* assuming that the stretch is uniform along the chain contour length and an explicit function  $\lambda(t)$  of the observation time, which operates on the orientational configuration resulting from the integration over the orientation history, the extra stress tensor is given by

$$\boldsymbol{\sigma}(t) = \lambda^2(t) \int_{-\infty}^t m(t-t') \mathbf{S}_{\text{DE}}^{\text{IA}}(t, t') dt' \quad (7)$$

Eq. (7) generated the necessity to find a stretch evolution equation, and a vast variety of concepts based on different kinetic ideas have been proposed in recent years (see *e.g.* Doi, 1980; McLeish and Larson, 1998; Mead *et al.*, 1998).

While in models with pre-averaged stretch the tube diameter is invariably assumed to stay constant and equal to its equilibrium value  $a_0$ , stretch can also be introduced by the assumption of a strain-dependent tube diameter, as first suggested by Marrucci and de Cindio (1980). In this way, also the pre-averaging of the stretch can be avoided, which is inherently present in models based on Eq. (7) or its differential approximations. It should also be noted that Eq. (7) with any function  $\lambda^2(t)$  is not in agreement with experimental results of reversed elongational flow of a monodisperse polystyrene melt (Nielsen and Rasmussen, 2008).

#### 5. The Molecular Stress Function Model

A generalized tube model with strain-dependent tube diameter was presented by Wagner and Schaeffer (Wagner and Schaeffer, 1992; 1993; 1994). In the Molecular Stress Function (MSF) model, tube segment stretch  $f$  is directly related to the tube diameter  $a$ , which decreases from its equilibrium value  $a_0$  with increasing stretch. Taking into account that the tube diameter  $a$  represents the mean field of the surrounding chains, it is assumed that the tube diameter is independent of the orientation of tube segments. The

extra stress is then given as

$$\boldsymbol{\sigma}(t) = \int_{-\infty}^t m(t-t') f^2 \mathbf{S}_{DE}^{IA}(t, t') dt' \quad (8)$$

The molecular stress function  $f = f(t, t')$  is the inverse of the relative tube diameter,

$$f(t, t') = a_0/a(t, t') \quad (9)$$

In contrast to Eq. (7), stretch in Eq. (8) does not only depend on the observation time  $t$ , but depends on the strain history, *i.e.* for time-dependent strain histories, chain segments with long relaxation times (*i.e.* at the center of the chain) see higher stretches than chain segments with short relaxation times (*i.e.* at the chain ends).

Following conventional arguments (Pearson *et al.*, 1989) and assuming that the affine deformation of the chain is balanced by a linear spring force, the evolution equation for  $f$  takes the form

$$\frac{\partial f}{\partial t} = f(\boldsymbol{\kappa} : \mathbf{S}) - \frac{1}{\tau_R} (f-1) \quad (10)$$

with velocity gradient  $\boldsymbol{\kappa}$  and a Rouse stretch relaxation time  $\tau_R$  of the chain. For PS390K, a value of  $\tau_R = 329$ s is obtained from Eq. (1). As demonstrated in Fig. 1, this does clearly not describe the steady-state elongational viscosity of PS390K. It is obvious from Fig. 1 that a linear spring force will quench chain stretch as long as the Weissenberg number  $Wi = \dot{\epsilon} \tau_R$  is much smaller than 1, while chain stretch will diverge in the limit of  $Wi \rightarrow 1$ , resulting in a diverging steady-state elongational viscosity. This is clearly seen by setting the left hand side of Eq. (10) to zero, which gives the maximum stretch  $f_{\max}$  as

$$f_{\max} = \frac{1}{1-Wi} \quad (11)$$

## 6. The Interchain Pressure Term and the Evolution Equation of Chain Stretch

Considering a chain composed of  $N$  Kuhn segments of length  $b$ , confined within a box of dimensions  $L_x$ ,  $L_y$  and  $L_z$ , where the overall length of the chain is much larger than the dimensions of the confining box, Doi and Edwards (1986) demonstrated that the pressure exerted by the chain on the walls of the box is anisotropic, if the chain is confined to an anisotropic box. The pressure acting on a box wall normal to the  $x$ -axis is given by the gradient of free energy  $A$  in the  $x$ -direction (Doi and Edwards, 1986),

$$P_x = -\frac{1}{L_y L_z} \frac{\partial A}{\partial L_x} = \frac{\pi^2 N b^2 k_B T}{3 L_x^2 V} \quad (12)$$

*i.e.* the pressure is increasing with increasing confinement of the chain. Taking  $z$  as the direction of the tube axis, and  $x$  and  $y$  as the directions perpendicular to the tube axis, and

setting  $L_x \approx L_y \approx a$  and  $V = a^2 L_{\text{Tube}}$ , this leads to (Marrucci and Ianniruberto (2004))

$$P_x = P_y \approx kT \frac{N b^2}{a^4 L_{\text{Tube}}} \quad (13)$$

As  $N b^2$  is a constant, and considering that the tube surface area being proportional to  $a L_{\text{Tube}}$  is constant even at large deformations (Wagner and Schaeffer, 1992), the relative radial pressure  $p/p_0$  will increase inverse proportionally to the 3rd power of the tube diameter  $a$  from its equilibrium value  $p_0$ ,

$$\frac{p}{p_0} = \frac{a_0^3}{a^3} \quad (14)$$

Therefore, when the tube diameter is decreased with increasing deformation, the radial pressure of the chain exerted on the surrounding topological constraints is increasing. Marrucci and Ianniruberto (2004) assumed that this radial pressure increase is balancing tube diameter reduction and thereby chain stretch. Considering elongational flow with strain rate  $\dot{\epsilon}$ , they derived a scalar evolution equation for the tube diameter  $a$ ,

$$\frac{\partial a}{\partial t} = -\dot{\epsilon} a + \frac{a_0}{\tau_a} \left( \frac{a_0^3}{a^3} - 1 \right) \quad (15)$$

We called  $\tau_a$  the tube diameter relaxation time (Wagner *et al.*, 2005), and replaced the first term on the right hand side of equation (15) by the general tensorial description for the deformation rate in analogy to equation (10) above (see *e.g.* Wagner *et al.* (2001)), which leads to

$$\frac{\partial a}{\partial t} = -(\boldsymbol{\kappa} : \mathbf{S}) a + \frac{a_0}{\tau_a} \left( \frac{a_0^3}{a^3} - 1 \right) \quad (16)$$

Inserting the definition of the molecular stress function,  $f = a_0/a$ , we obtained from Eq. (16) the following evolution equation for the tension in a chain segment,

$$\frac{\partial f}{\partial t} = f(\boldsymbol{\kappa} : \mathbf{S}) - \frac{f^2 (f^3 - 1)}{\tau_a} \quad (17)$$

with the initial condition  $f(t=t', t') = 1$ . When the linear-viscoelastic response is known, Eq. (17) together with Eq. (8) represent a full constitutive relation with only one material parameter, the tube diameter relaxation time  $\tau_a$ .

Due the nonlinear restoring pressure term on the right hand side of Eq. (17), the divergence of the maximum stretch  $f_{\max}$  in constant strain-rate elongational flow is now removed, and for fast deformations, the steady-state elongational viscosity scales with

$$\eta_{us} = \sqrt{\tau_a} \dot{\epsilon}^{-\frac{1}{2}} \quad (18)$$

in good agreement with the experimental results of Bach *et al.* (2003) and the analysis of Marrucci and Ianniruberto (2004). The tube diameter relaxation time is expected to be

proportional to the Rouse relaxation time. However, the exact value of the proportionality constant remained elusive, and  $\tau_a$  was so far considered as a fit parameter. As shown in Fig. 1, the steady-state elongational viscosity as predicted from Eqs. (8) and (17) for PS390K is in excellent agreement with the data, when the value of the tube diameter relaxation time is fitted to  $\tau_a = 1462$  s.

## 7. Relation of Tube Diameter Relaxation and Rouse Time

Rewriting Eq. (17) in the form

$$\frac{\partial f}{\partial t} = f(\kappa : \mathbf{S}) - \frac{f-1}{\tau_a} [3 + 9(f-1) + 10(f-1)^2 + 5(f-1)^3 + (f-1)^4] \quad (19)$$

it is obvious that in first order in the stretch, *i.e.* for  $f-1 \ll 1$ , Eq. (17) reduces to the classical relation (10) with

$$\frac{\partial f}{\partial t} = f(\kappa : \mathbf{S}) - \frac{f-1}{\tau_a/3} \quad (20)$$

*i.e.* in the limit of small stretch, the tube diameter relaxation time  $\tau_a$  of the melt can be identified with

$$\tau_a = 3 \tau_R \quad (21)$$

This is an important result. However, in view of the fact that in the case of small chain stretch, tube segment length and tube diameter are nearly equal, and therefore the effect of the chain pressure on the tube wall corresponds to the tension along the chain, this result is not as surprising as it may seem at first.

In the development of evolution equations for chain stretch until now, two different approaches have been followed: In the classical relation (10), chain stretch is assumed to be balanced by the spring force of the chain in the longitudinal (stretched) direction of the tube, leading to a stretch relaxation term with Rouse time  $\tau_R$ . On the other hand, Marrucci and Ianniruberto (2004) assume that the interchain pressure resulting from tube diameter reduction and acting in the two dimensions perpendicular to the tube, is responsible for balancing further tube diameter reduction and thereby chain stretch as described by Eqs. (16) and (17). Thus, while in the classical relation (10), force balance is restricted to the longitudinal direction of the tube, the interchain tube pressure approach of Eq. (15) considers only force balance in the lateral direction of the tube. The original findings of Doi and Edwards (1986), however, maintain that the chain pressures on the walls of a confining box are anisotropic if the dimensions of the box are anisotropic, *i.e.* there will be different restoring forces in the longitudinal direction (no wall) and in the lateral direction of the tube, where the chain is confined by topological constraints of the other chains. We therefore argue that chain stretch is balanced simultaneously and additively by

two restoring tensions with weights of 1/3 in the longitudinal direction and 2/3 in the lateral direction, leading to an evolution equation for the stretch of the form

$$\frac{\partial f}{\partial t} = f(\kappa : \mathbf{S}) - \frac{1}{3} \frac{f-1}{\tau_R} - \frac{2}{3} \frac{f^2(f^3-1)}{\tau_a} \quad (22)$$

or, by use of Eq. (21)

$$\frac{\partial f}{\partial t} = f(\kappa : \mathbf{S}) - \frac{f-1}{3 \tau_R} \left[ 1 + \frac{2}{3} f^2 (f^2 + f + 1) \right] \quad (23)$$

Eq. (23) is equivalent to the classical relation (10) in first order in the stretch. It removes the singularity present in the classical relation (10) for  $Wi = \dot{\epsilon} \tau_R \rightarrow 1$ . It does not contain any nonlinear material parameter, as the Rouse time  $\tau_R$  of the chain is determined by the molecular characteristics of the polymer as obtained from linear viscoelasticity, and thus we have made significant progress in developing a nonlinear integrodifferential constitutive relation, Eqs. (8) and (23), with no free parameters.

As the interchain pressure term of Marrucci and Ianniruberto (2004) enters in Eq. (22) with the weight of 2/3, the effective tube diameter relaxation time  $\tau_{eff}$  of the melt at large stretches is

$$\tau_{eff} = \frac{9}{2} \tau_R \quad (24)$$

This can be seen from Eq. (23) by considering that at large  $f$ , the stretch is determined mainly by the interchain pressure term. The factor 9/2 is in good agreement with the findings of Wagner *et al.* (2005) for PS melts with molar masses of 200 kg/mol and 390 kg/mol, for which, as seen from Table 1, a factor of 4.2 and 4.4, respectively, between  $\tau_a$  and  $\tau_R$  was found.

## 8. Comparison of MSF Modeling with Experimental Data

### 8.1. Elongational Flow

To demonstrate the validity of the stretch evolution equation based simultaneously on interchain pressure and Rouse relaxation, we reanalyze the data of Bach *et al.* (2003). Figs. 2(a) and 2(b) present comparisons of the transient elongational viscosity data for PS 390K and PS 200K to predictions of Eqs. (8) and (23). The time-dependent increase as well as the plateau value of the elongational viscosities is seen to be in excellent agreement for both polystyrene samples with the predictions of the stretch evolution equation (23). It should be noted that this agreement is achieved by use of a single material parameter, the Rouse stretch relaxation time  $\tau_R$ , which is determined by the molecular characteristics of the polymer and is obtained from linear viscoelasticity.

In Fig. 3, the steady-state elongational viscosities of

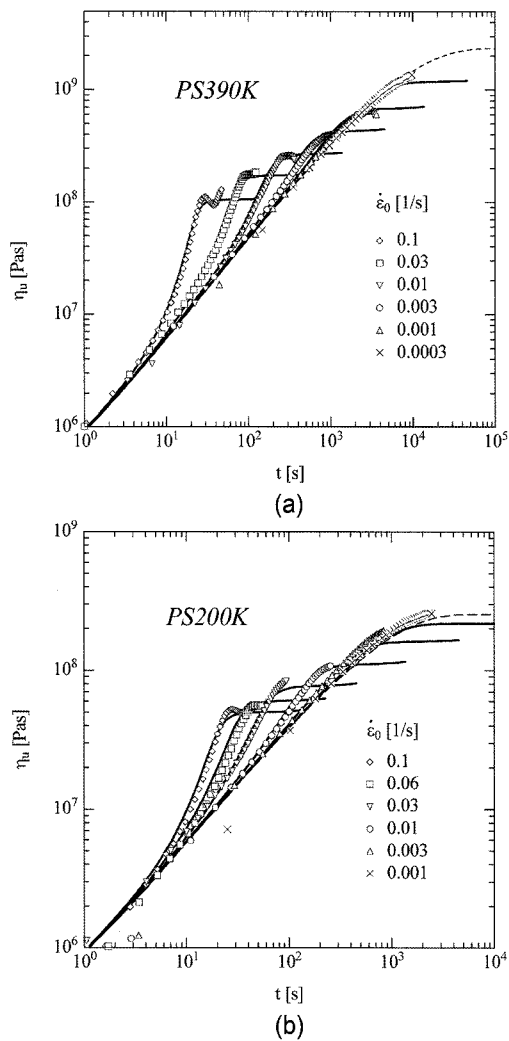


**Fig. 2.** Comparison of measured transient elongational viscosity data (symbols) to predictions (full lines) by MSF model with stretch evolution equation (23) and Rouse times  $\tau_R$  as given in Table 1. Dotted line indicates  $\eta_{u0}(t)$ .

PS390K and PS200K as predicted by Eqs. (8) and (23) are presented and compared to the experimental data, and excellent agreement is observed.

## 8.2. Shear Flow

Comparison of shear viscosity data obtained for a series of SBR copolymer melts (Boukany *et al.* 2009) and predictions of the MSF model are presented in Figs. 4(a)-(d) for SBR100K, SBR170K, SBR250K and SBR500K, respectively. As expected, the shear viscosity data confirm a negative deviation from the linear-viscoelastic start-up prediction, which is the stronger the higher the shear rate applied, *i.e.* the melts show strong shear thinning. A maximum in the shear viscosity data is also revealed, before the shear thinning itself occurs. These features are described remarkably well by the MSF model, and general agreement between experimental data and predictions of the MSF

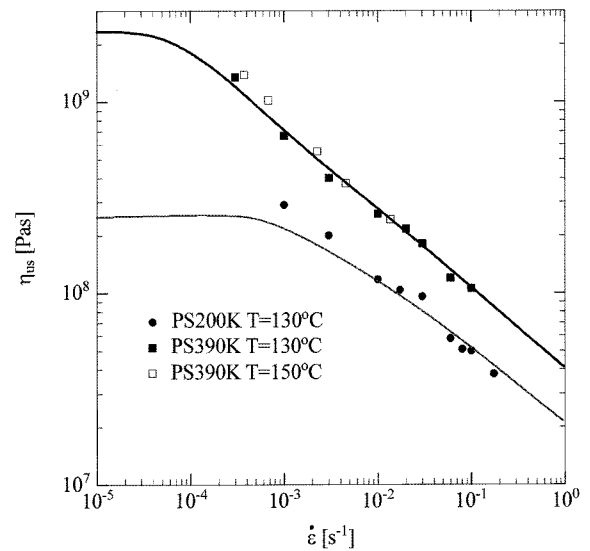
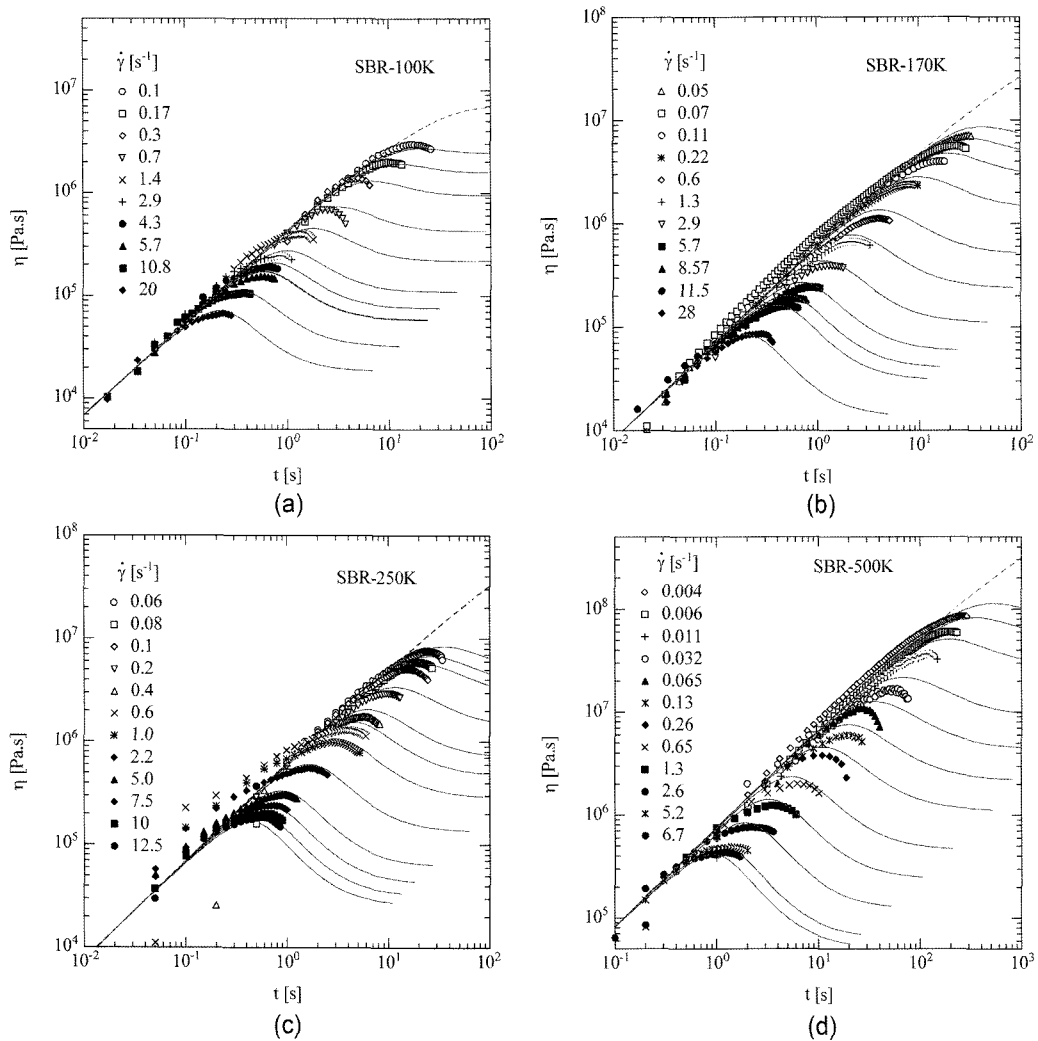


**Fig. 3.** Comparison of measured steady-state elongational viscosity data of PS390K and PS200K (symbols) to predictions (lines) of MSF model with stretch evolution equation (23) and Rouse relaxation times  $\tau_R$  as given in Table 1.

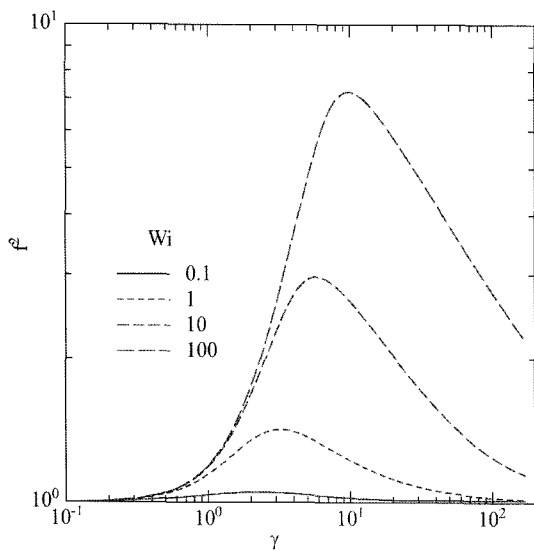
model is observed for all four SBR samples considered and for a wide range of shear rates. The disagreements between data and model at low values of the shear rate in the case of SBR170K, SBR250K and SBR500K may have their origin in inaccuracies of the experimentally determined linear-viscoelastic spectra with the terminal relaxation times of these melts not being fully resolved. There are no experimental data at times much beyond the time of the maximum shear viscosity, and therefore there are no data for comparison with predicted steady-state shear viscosities. Particle-tracking velocimetry (PVT) in start-up shear flows has revealed that the shear field becomes inhomogeneous in space at times after the shear stress overshoot due to shear banding, a stratification that remains even in the regime where the shear viscosity is expected to show a stationary value (Tapadia and Wang, 2006).

Fig. 5 presents the square of stretch,  $f^2$ , as a function of shear deformation  $\gamma$  as predicted by the MSF model, and it is seen that the stretch of the molecular chains increases with the intensity of the flow, *i.e.* with the Weissenberg number  $Wi = \dot{\gamma} \tau_R$  based on the Rouse time. It is also observed that the maximum in the stretch is not only increasing with increasing shear rate, but is also shifted to higher shear deformations with increasing Weissenberg number, which, in turn leads to a shift of the maximum of the shear viscosity to higher shear deformations with increasing shear rates.

The maximum of the shear viscosity,  $\gamma_{max}$ , is plotted as a function of the Weissenberg number in Fig. 6 for the SBR melts indicated by their average number of entanglements per chain,  $Z = M_w/M_e$ . The values of  $Z$  given are those reported by Boukany *et al.* (2009). A constant value of



**Fig. 4.** Comparison of measured transient shear viscosity data (symbols) of SBR 100K, 170K, 250K and 500K at  $T=23^\circ\text{C}$  to predictions (full lines) by MSF model with stretch evolution equation (23). Dotted line indicates  $\eta_0(t)$ .



**Fig. 5.** Comparison of the square of relative chain stretch,  $f^2$ , as a function of deformation for different Weissenberg numbers  $Wi = \dot{\gamma} \tau_R$  based on the Rouse time.

$\gamma_{\max} = 2.1$ , irrespective of shear rate, is predicted by the DE model (Doi and Edwards 1979). When molecular chains are increasingly stretched with increasing shear rates, *i.e.* for  $Wi > 1$ ,  $\gamma_{\max}$  increases according to a power-law. This behaviour is independent of the number of entanglements and scales with the Rouse time. If the classical Rouse stretch model, Eq. (10), is considered, the experimental data are clearly overpredicted, while the MSF model, within experimental error, describes the data correctly up to Weissenberg numbers of  $Wi \approx 30$ . This comparison clearly reflects the importance of taking the stretch of polymer chains correctly into account.

## 9. Conclusions

The pressures exerted by a polymer chain on the walls of an anisotropic confinement are anisotropic (Doi and Edwards, 1986). Implementation of these findings into a tube model with variable tube diameter leads to an interchain pressure

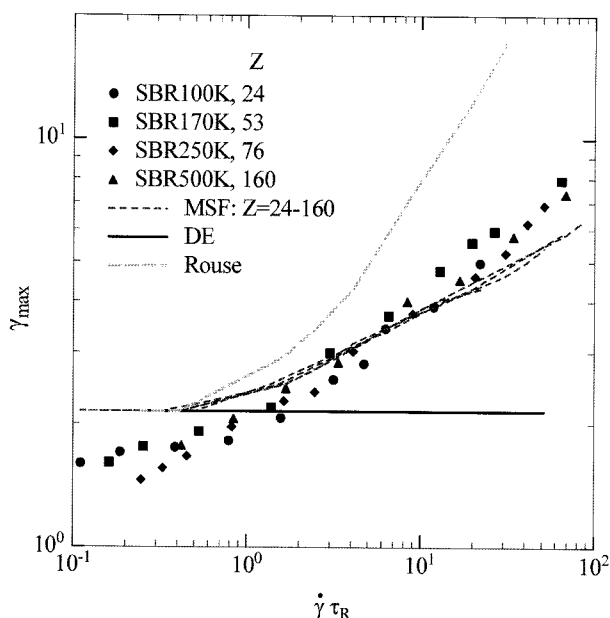


**Fig. 6.** Comparison of measured shear deformation at maximum shear stress (symbols) as a function of Weissenberg number to predictions by MSF model with stretch evolution equation (23) (short-dashed lines), DE model (continuous line), Eq. (3), and Rouse stretch (long-dashed line), Eq. (10), for SBR samples.

term in the lateral direction of the tube, which is inverse proportional to the 3<sup>rd</sup> power of the tube diameter  $a$  (Marrucci and Ianniruberto, 2004). When the tube diameter is decreased with increasing deformation, the chain is stretched, and the radial pressure of the chain exerted on the surrounding topological constraints is increased and resists further tube diameter reduction. This concept leads to an evolution equation for the chain stretch with an inter-chain pressure term that is characterized by a tube diameter relaxation time  $\tau_a$  (Wagner *et al.*, 2005).

The tube diameter relaxation time  $\tau_a$  of the melt was shown to be equal to 3 times the Rouse time  $\tau_R$  of the chain by considering small chain stretch, when tube segment length and tube diameter are still nearly equal, and the effect of the interchain pressure term in lateral direction is equal to the relative tension of the chain in the longitudinal direction of the tube.

At larger deformations, the equality between the inter-chain pressure in the lateral direction (being inverse proportional to the 3<sup>rd</sup> power of the tube diameter  $a$ ) and the tension in the longitudinal direction (increasing linearly with stretch) does no longer hold. Chain stretch is then balanced by two restoring tensions with weights of 1/3 in the longitudinal direction and 2/3 in the lateral direction, both of which are characterized by the Rouse relaxation time. This approach is in quantitative agreement with the elongational behavior of two monodisperse polystyrene melts with molar masses of  $M_w = 200,000\text{g/mol}$  and  $390,000\text{g/mol}$

as determined by Bach *et al.* (2003) and Hassager (2004), as well as the shear flow data of four nearly monodisperse SBR copolymer melts (Boukany *et al.*, 2009). In the case of shear, agreement is excellent up to and somewhat beyond the maximum in the shear viscosity, when shear banding begins to corrupt experimental data. The MSF model is also in good agreement with the shear deformation  $\gamma_{\max}$  at the maximum value of the shear viscosity observed up to Weissenberg numbers of  $Wi \approx 30$ , although the slope of the power-law increase in  $\gamma_{\max}$  with increasing Weissenberg number observed is somewhat higher than predicted. This may be due to experimental issues at high shear rates, or to the effect of glassy modes not taken into account by the model.

In conclusion, the analysis of experimental data in elongational and shear flow of monodisperse linear polystyrene and SBR melts clearly demonstrates that the tube, *i.e.* the confinement of a test chain, is characterized by the orientation in the direction along the tube, and the diameter of the tube in the lateral dimension. Chain stretch is associated with a reduction of the tube diameter, which is balanced by a linear spring force in the longitudinal direction and a nonlinear interchain pressure in the lateral direction, both of which are governed by the Rouse time of the chain. Thus for the first time a constitutive equation is available which allows quantitative modeling of nonlinear extension and shear rheology of monodisperse linear polymer melts exclusively based on linear-viscoelastic characterization.

## Acknowledgments

We thank A. Bach, J.K. Nielsen, H.K. Rasmussen, O. Hassager, P.E. Boukany, S.Q. Wang, and X. Wang for sharing their experimental data with us. Financial support from the German Science Foundation (DFG) is gratefully acknowledged.

## References

- Bach, A., K. Almdal, H.K. Rasmussen and O. Hassager, 2003, "Elongational viscosity of narrow molar mass distribution polystyrene," *Macromolecules* **36**, 5174-5179.
- Boukany P.E., S.Q. Wang and X. Wang, 2009, "Universal scaling behavior in startup shear of entangled linear melts", *J. Rheol.* **53**, 617-629.
- Doi, M., 1980, "A constitutive equation derived from the model of Doi and Edwards for concentrated polymer solutions and polymer melts, *J. Polym. Sci. B Phys. Ed.* **18**, 2055-2067.
- Doi, M. and Edwards, S.F., 1979, Dynamics of Concentrated Polymer Systems. Part 4.- Rheological Properties. *Trans. Faraday Soc II* **75**, 38-54.
- Doi, M. and S. F. Edwards, 1986, *The Theory of Polymer Dynamics*, Oxford University Press, Oxford.
- Hassager, O., 2004, "Polymer fluid mechanics: Molecular orientation and stretching," Proc. XIVth Int. Congress on Rheo-



- ology, **NF01**.
- Isaki, T., M. Takahashi and O. Urakawa, 2003, "Biaxial damping function of entangled monodisperse polystyrene melts: Comparison with the Mead-Larson-Doi model," *J. Rheol.* **47**, 1201-1210.
- Marrucci, G. and B. de Cindio, 1980, "The stress relaxation of molten PMMA at large deformations and its theoretical interpretation," *Rheol. Acta* **19**, 68-75.
- Marrucci, G. and G. Ianniruberto, 2004, "Interchain pressure effect in extensional flows of entangled polymer melts," *Macromolecules* **37**, 3934-3942.
- McLeish, T.C.B. and R.G. Larson, 1998, "Molecular constitutive equations for a class of branched polymers: the pom-pom polymer," *J. Rheol.* **42**, 81-110.
- Mead, D.W., R.G. Larson and M. Doi, 1998, "A molecular theory for fast flows of entangled polymers," *Macromolecules* **31**, 7895-7914.
- Menezes, E.V. and W.W. Graessley, 1982, "Nonlinear rheological behavior of polymer systems for several shear-flow histories," *Polym. Phys.* **20**, 1817-1833.
- Nielsen J.K., H.K. Rasmussen, O. Hassager and G.H. McKinley, 2006, "Elongational viscosity of monodisperse and bidisperse polystyrene melts," *J. Rheol.* **50**, 453-476.
- Nielsen J.K., H.K. Rasmussen, and O. Hassager, 2008, "Stress relaxation of narrow molar mass distribution polystyrene following uniaxial extension," *J. Rheol.* **52**, 885-899.
- Nielsen J.K. and H.K. Rasmussen, 2008, "Reversed extension flow," *J. Non-Newtonian Fluid Mech.* **155**, 15-19.
- Osaki, K., K. Nishizawa and M. Kurata, 1982, "Material time constant characterizing the nonlinear viscoelasticity of entangled polymeric systems," *Macromolecules* **15**, 1068-1071.
- Pearson, D.S., A. Kiss, L. Fetters and M. Doi, 1989, "Flow-Induced Birefringence of Concentrated Polyisoprene Solutions," *J. Rheol.* **33**, 517-535.
- Takahashi, M., T. Isaki, T. Takigawa and T. Masuda, 1993, "Measurement of biaxial and uniaxial extensional flow behavior of polymer melts at constant strain rates," *J. Rheol.* **37**, 827-846.
- Tapadia, P. and S.Q. Wang, 2006, "Direct visualization of continuous simple shear in non-newtonian polymeric fluids", *Phys. Rev. Lett.* **96**, 016001.
- Wagner, M.H. and J. Schaeffer, 1992, "Nonlinear strain measures for general biaxial extension of polymer melts," *J. Rheol.* **36**, 1-26.
- Wagner, M.H. and J. Schaeffer, 1993, "Rubbers and Polymer melts: Universal aspects of non-linear stress-strain relations," *J. Rheol.* **37**, 643-661.
- Wagner, M.H. and J. Schaeffer, 1994, "Assessment of non-linear strain measures for extensional and shearing flows of polymer melts," *Rheol. Acta.* **33**, 506-516.
- Wagner, M.H., P. Rubio and H. Bastian, 2001, "The molecular stress function model for polydisperse and polymer melts with dissipative convective constraint release," *J. Rheol.* **45**, 1387-1412.
- Wagner, M.H., S. Kheirandish and O. Hassager, 2005, "Quantitative prediction of transient and steady-state elongational viscosity of nearly monodisperse polystyrene melts", *J. Rheol.* **49**, 1317-1327.